Fibers **2015**, *3*, 523-538; doi:10.3390/fib3040523

OPEN ACCESS

fibers

ISSN 2079-6439

www.mdpi.com/journal/fibers

Article

The Influence of Solid-State Drawing on Mechanical Properties and Hydrolytic Degradation of Melt-Spun Poly(Lactic Acid) (PLA) Tapes

Fang Mai [1], Wei Tu [2], Emiliano Bilotti [1,2] and Ton Peijs [1,2,*]

[1] School of Engineering and Materials Science, Queen Mary University of London, Mile End Road, E1 4NS London, UK; E-Mails: f.mai@qmul.ac.uk (F.M.); e.bilotti@qmul.ac.uk (E.B.)

[2] Nanoforce Technology Ltd., Joseph Priestley Building, Queen Mary University of London, Mile End Road, E1 4NS London, UK; E-Mail: w.tu@nanoforce.co.uk

* Author to whom correspondence should be addressed; E-Mail: t.peijs@qmul.ac.uk; Tel.: +44-020-7882-8865.

Academic Editor: Stephen C. Bondy

Received: 21 September 2015 / Accepted: 13 November 2015 / Published: 1 December 2015

Abstract: The influence of solid-state drawing on the morphology of melt-spun poly(L-lactic acid) (PLLA) tapes, and the accompanying changes in mechanical and degradation behaviour have been studied. Mechanical properties are found to be strongly dependent on both applied draw ratio and drawing temperature. Moduli of these highly oriented tapes are significantly increased compared to as-extruded tapes at both ambient and elevated temperatures. Interestingly, drawing leads to a significant increase in elongation to break (~3 times) and toughness (~13 times) compared to as-extruded tapes. Structural and morphological characterization indicates strain-induced crystallization as well as an increase in orientation of the crystalline phase at small strains. Upon further stretching, an "overdrawing" regime is observed, with decreased crystalline orientation due to the breakage of existing crystals. For fixed draw ratios, a significant increase in Young's modulus and tensile strength is observed with increasing drawing temperature, due to a higher crystallinity and orientation obtained for tapes drawn at higher temperatures. FT-IR results indicate no crystal transformation after drawing, with the α-form being observed in all tapes. Hydrolytic degradability of PLLA was significantly reduced by solid-state drawing.

Keywords: poly(lactic acid); fibres; morphology; mechanical properties; degradation

1. Introduction

Poly(lactic acid) (PLA), which is produced from annually renewable resources such as corn and sugar beets, has attracted great interest as a sustainable and environmental-friendly bioplastic. However, the lack of performance limits its application mainly to disposables and packaging, rather than more demanding engineering applications. The addition of cellulose and more recently nanocellulosic fillers represents one way to improve the physical properties of these bioplastics [1], while depending upon the nature and characteristics of the nanoparticles used, the ultimate properties of the resulting nanocomposite materials can be tailored [2].

In polymer materials high strength and stiffness can also be achieved by orientating polymer chains to create highly anisotropic structures like fibres, films, or tapes. Oriented polymer fibres have been an important topic of research since the 1970s [3]. Successful commercial examples of high performance polymer fibres include ultra-high molecular weight polyethylene (UHMWPE) as commercialized under the name Dyneema® [4] and aramid fibres as commercialized under the names Kevlar® and Twaron® [5].

The most commonly used methods of producing PLA fibres are melt spinning and solution spinning. In general, solution-spun fibres are superior to melt-spun fibres from the standpoint of mechanical properties. This is attributed to the lower chain entanglement of polymer molecules in the solution state as compared to the melt state. For instance, Penning *et al.* [6] reported that solution spinning followed by hot drawing resulted in low crystallinity fibres having a tensile strength of 1 GPa, whereas fibres prepared from melt spinning followed by hot drawing had considerably lower strengths, ranging from 0.19 GPa for completely amorphous copolymers to 0.53 GPa for PLA homopolymer. Fambri *et al.* [7] were able to obtain fibres with tensile strengths and moduli of 1.1 GPa and 10 GPa, respectively, using a Purac grade biomedical material having M_v = 660,000. Similarly, Leenslag *et al.* [8] produced fibres with a tensile strength and modulus of 2.1 GPa and 16 GPa from PLLA with M_v = 900,000, using a solution spinning process. The main drawbacks of this process are that solvents such as chloroform and toluene are necessary, while production speeds are rather low.

Commercial PLA fibres are generally produced using a melt spinning technique. Generally, PLA fibres are produced by a two-stage process: first melt extrusion followed by hot drawing. Eling *et al.* [9] reported melt extrusion of PLLA at 185 °C through a capillary, followed by hot drawing in a tube furnace. The obtained fibres had a modulus of 7 GPa and a tensile strength of 0.5 GPa. The investigation of Cicero *et al.* [10] illustrates two-step melt spinning of textile grade PLA. A maximum modulus and tensile strength of 3.2 GPa and 0.38 GPa were obtained respectively. Later, Cicero *et al.* [11] investigated the crystalline morphology of PLA by small-angle X-ray scattering and atomic force microscopy. They proposed a representation of the molecular structure of PLA where the alignment of microfibres along the fibre axis is determined by the draw ratio. The crystalline and amorphous regions form stacks within the microfibrils and the interfibrillar region is populated by amorphous chains.

PLA filaments can be spun at high-speed take-up velocities of up to 5000 $m \cdot min^{-1}$ [12]. The crystallinity, birefringence, tensile strength, Young's modulus, and yield strength all exhibit maxima at take-up speeds between 2000 and 3000 $m \cdot min^{-1}$. The boiling water shrinkage exhibits a minimum in this range, indicating that a stable morphology is developed through stress-induced crystallization. A maximum tensile strength of the as-spun filaments has been reported of 385 MPa with a maximum modulus of 6 GPa.

This paper is concerned with the understanding of structure-property relationships of PLLA films and tapes, rather than fibres, during stretching to optimize its use properties via processing. Since PLLA is a semi-crystalline polymer, its mechanical properties depend strongly on its crystallinity, crystal orientation, and morphology. Hence, the influence of draw ratio and drawing temperature on the superstructure (orientation and crystallization, *etc.*) and morphology evolution of PLLA, and the accompanying changes in mechanical and degradation properties will be discussed.

2. Experimental Section

2.1. Materials

PLLA (NatureWorks® Ingeo™ 4032D), containing 2.2% of D-isomer units, was purchased from Resinex (Buckinghamshire, UK). Gel permeation chromatograph (GPC) in chloroform showed that the number average molecular weight (M_n) of the as received polymer is 133,500 g·mol^{-1}. The melting temperature (T_m) is approximately 169 °C as measured by differential scanning calorimetry (DSC, Mettler-Toledo 822e, Leicester, UK).

2.2. Manufacture of PLLA Tapes

Figure 1 shows the tape production line schematically. A single screw extruder (Dr. Collin GmbH, TEACH-LINE® E 20T) with a length to diameter screw ratio (L/D) of 25:1 and a compression ratio of 2.85:1 was employed to obtain PLLA extruded films. Default extrusion settings are described in Table 1. Molten polymer was extruded through a 50 mm slit die. These extruded films were quenched on a chill roll, followed by post-drawing on heated rollers (Dr. Collin GmbH, TEACH-LINE® MDO) to create an oriented tape. These tapes were drawn in a two-step solid-state drawing process below the melting temperature. The first drawing step provided some initial orientation, but ultimate drawing was performed in the second step. The total draw ratio (*DR*) is defined as the ratio of drawn tape length to original tape length. The *DR* of as-extruded tape is 1. The temperature of the first set of rollers and initial draw ratio were fixed, while the second drawing conditions were varied for this investigation. The drawing parameters are listed in Table 2.

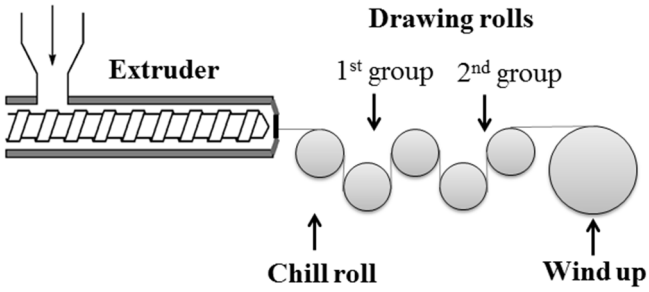

Figure 1. Schematic of extrusion and solid-state drawing pilot-production line.

Table 1. Default extrusion parameters.

Process	Temperature (°C)							Screw Speed (rpm)
	Zone 1	Zone 2	Zone 3	Zone 4	Zone 5	Zone 6	Tube	
Extruder	170	165	210	215	210	200	205	20

Table 2. Solid-state drawing parameters (to give different *DR*).

Process	Temperature (°C)	Roller speed (1st Group)	Roller Speed (2nd Group)
1st drawing	80	0.5 m·min^{-1}	2 m·min^{-1}
2nd drawing	70/90/110/130	0.2 m·min^{-1}	0.8 m·min^{-1}

2.3. Characterization

Number average molecular weight (M_n) was determined by gel permeation chromatography (GPC, Agilent Technologies, Cheshire, UK). Measurements were performed at 30 °C in chloroform with an AGILENT Technologies 1200 series, equipped with 2× Agilent PLgel Mixed D column and a pre-column. Then, 200 mL of polymer solution with a concentration of 5 mg·mL^{-1} was injected at 1 mL·min^{-1}. The molar masses were calculated using a polystyrene standard. Morphological studies were carried out on gold-coated samples using scanning electron microscopy (SEM) (FEI Inspector-F, Eindhoven, The Netherlands). Differential scanning calorimetry (DSC) was run in a Mettler-Toledo 822e. For all measurements, the samples were heated to 200 °C at 10 °C·min^{-1} under a N_2 atmosphere. The degree of crystallization (X_c) was calculated using the 100% crystalline PLLA enthalpy (93.6 J·g^{-1}) [13]. Fourier transform infrared (FT-IR) spectra of various samples were measured with a Bruker Tensor 27 spectrometer. Attenuated total reflectance (ATR) mode was taken for the IR measurement. The spectra were obtained by collecting 16 scans at a 4 cm^{-1} resolution. OPUS software was used for data collection and analysis such as peak picking. The software recorded the IR spectrum in absorbance mode. The spectra were normalized to the same background and shifted vertically for comparison and clarity. No additional correction was applied. Wide-angle X-ray scattering (WAXS) were carried out at the BM26 beamline of the European Synchrotron Radiation Facility. The energy of the radiation source was 1.033 Å. The sample-detector distance was 138.6 mm. All the 2D patterns were corrected for background scattering, and then integrated into 1D intensity profiles using Fit2d Software. Tensile tests were performed using an Instron 5586 at room temperature, equipped with a 1 kN load cell. The reported values were calculated as averages over six specimens. Since the strain at break of as-extruded PLA tape was less than 20%, a lower testing crosshead speed (8 mm/min) was used. Rectangular shaped specimens were used for testing. The geometry of the test specimens is shown in Table 3. The thicknesses of the tapes decrease with drawing and increasing drawing temperatures. To cut the specimens to a width of around 10 mm, edges were removed with a razor blade, except for the tapes drawn at 130 °C to *DR* = 8. Since the width of these tapes is around 7 mm, the entire sample was used for tensile testing.

Table 3. Geometry of the specimens used for tensile testing.

Samples	Thickness (mm)	Width (mm)
As-extruded	0.182 ± 0.17	~10
90 °C *DR* = 4	0.094 ± 0.01	~10
90 °C *DR* = 5	0.093 ± 0.004	~10
90 °C *DR* = 8	0.079 ± 0.003	~10
70 °C *DR* = 8	0.091 ± 0.006	~10
110 °C *DR* = 8	0.059 ± 0.002	~10
130 °C *DR* = 8	0.055 ± 0.007	~7

Dynamic mechanical analysis (DMA) was performed on PLLA tapes of different draw ratios using a Q800 DMA from TA Instruments. Specimens were tested in tension mode. A gauge length of 15 mm was used. The system was cooled to −10 °C, and then heated to 150 °C at a rate of 3 °C·min^{-1}. A static force of 0.01 N was applied to ensure the tape was taut between the grips.

3. Results and Discussion

3.1. The Influence of Drawing on Mechanical Properties of PLLA Tapes

It is expected that mechanical properties will improve with increasing *DR* because of increasing strain-induced crystallization and orientation. Figure 2a shows typical stress-strain curves of the PLLA tape prepared at 90 °C upon different draw ratios. For drawn PLLA tapes, strain hardening is observed after yielding. This slope of the strain hardening is strongly related to the *DR*. Upon drawing four times, the slope of the strain hardening modulus actually jumps. The higher the *DR*, the greater the strain hardening of the tapes. This can be explained by the strain-induced crystallization and orientation. This strain-hardening behaviour is advantageous to industrial thermoforming processes because it assists in the production of higher quality films with uniform thickness [14]. As expected, drawing has a positive effect on the Young's modulus and tensile strength of the tapes. As shown in Figure 3a, compared to as-extruded PLLA tape (1.8 GPa in modulus and 53 MPa in tensile strength), a 128% and 227% increase in Young's modulus and tensile strength were achieved for oriented tapes of *DR* = 8 drawn at 90 °C (4.1 GPa in modulus and 174 MPa in tensile strength), respectively.

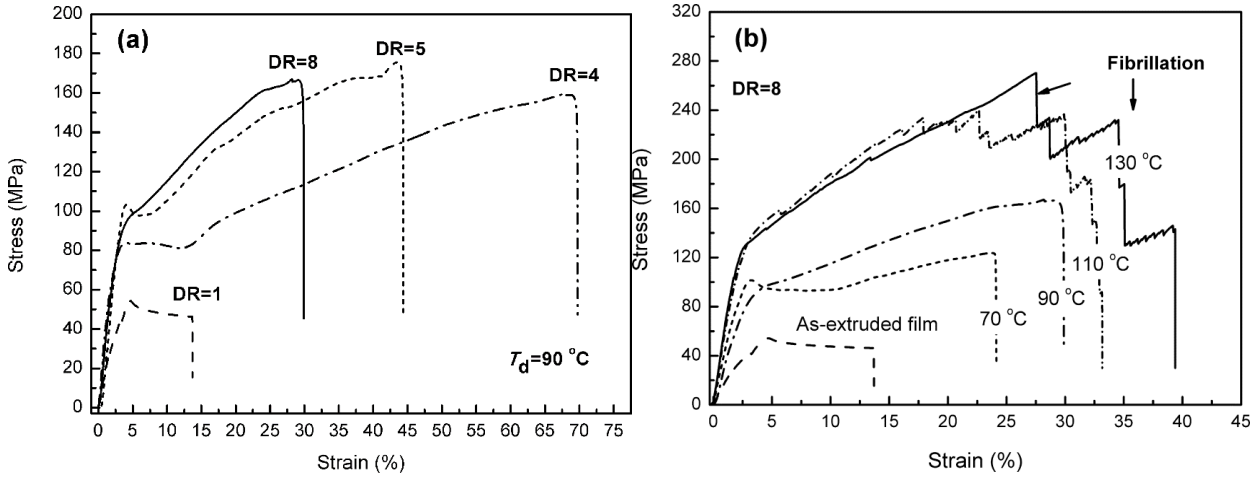

Figure 2. Stress-strain curves of poly(L-lactic acid) (PLLA) tapes subjected to (**a**) various draw ratios (T_d = 90 °C); and (**b**) different drawing temperatures (*DR* = 8).

The experimental results displayed in Figure 2b and Figure 3b show a significant effect of drawing temperature (T_d) on the mechanical properties of PLLA tapes drawn in the range of 70–130 °C. This dramatic influence has also been reported for polypropylene (PP) tapes [15]. The general tendency is that both Young's modulus and tensile strength of the post drawn tapes increases with T_d. The highest values of Young's modulus and tensile strength achieved are 6.7 GPa and 280 MPa, respectively, at a drawing temperature of 130 °C. Compared to as-extruded PLLA, a 3.7 and 5.2 times increase in Young's modulus and tensile strength is achieved.

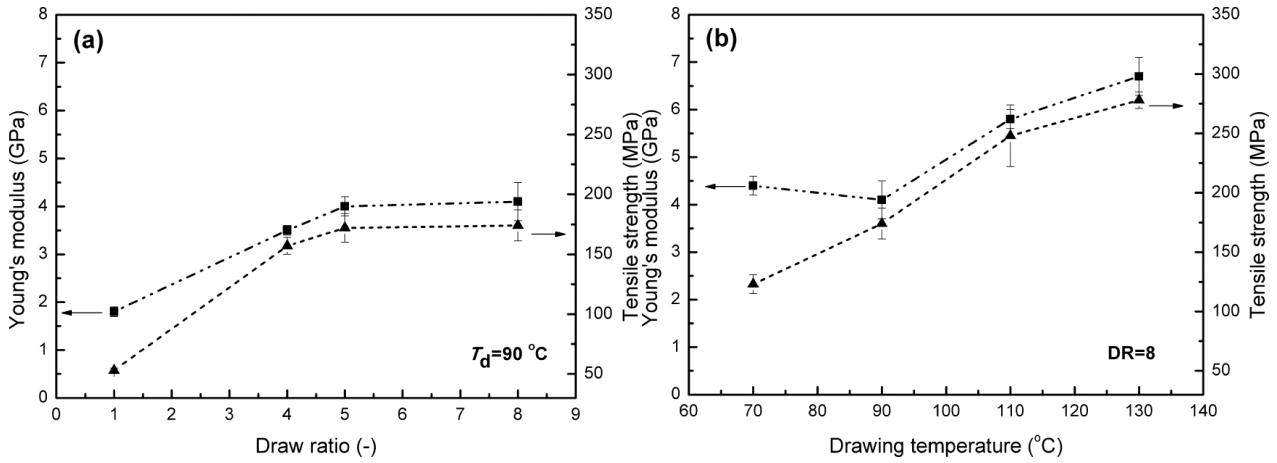

Figure 3. Young's modulus and tensile strength as a function of (**a**) draw ratio and (**b**) drawing temperature in the specimen.

Interestingly, compared to the brittle behaviour of as-extruded PLLA films, a much more ductile behaviour is observed for the drawn tapes (see Table 4). At T_d = 90 °C, the elongation to break and toughness first significantly increases at DR = 4 then slightly decreases when DR > 4. At a fixed DR = 8, both elongation to break and toughness increase with T_d. Compared to as-extruded PLLA, the elongation to break and toughness is increased by 220% and almost 1200% for tapes drawn at 130 °C. A possible reason for this improvement is that in these oriented tapes, growing cracks are arrested by the anisotropic microstructure; therefore, catastrophic failure is postponed [16]. However, another reason is probably related to the intrinsic deformation behaviour of PLA. Govaert and co-workers [17] showed that PLA exhibits a very strong post-yield softening behaviour together with virtually no strain hardening, the combination of both leading to strong localization of deformation and brittle fracture [18,19]. Mechanical pre-deformation as a result of drawing will lead to an increase in strain hardening due to orientation of crystalline material, which will alter the subtle interplay between strain softening and strain hardening. This will affect localisation of deformation, with an increase in strain hardening leading to less localization, more stable neck formation, and an increase in strain at break.

Table 4. Tensile properties of various PLLA tapes.

T_d (°C)	DR	Young's Modulus (GPa)	Tensile Strength (MPa)	Strain at Break (%)	Toughness * ($J \cdot m^{-3}$)
Extruded	1	1.8 ± 0.1	53 ± 2	12 ± 2	5.9×10^6
90	4	3.5 ± 0.1	157 ± 7	66 ± 9	8.3×10^7
90	5	4.0 ± 0.2	172 ± 12	42 ± 6	5.9×10^7
90	8	4.1 ± 0.4	174 ± 13	29 ± 3	3.8×10^7
110	8	5.8 ± 0.2	248 ± 26	33 ± 3	6.3×10^7
130	8	6.7 ± 0.4	278 ± 7	38 ± 3	7.5×10^7

Notes: * Toughness = $\int_0^{\varepsilon_f} \sigma d\varepsilon$, where σ is stress, ε is strain, and ε_f is the failure strain.

The maximum tensile modulus achieved in this work for tapes (6.7 GPa) compares well to the moduli previously reported for melt-spun drawn PLLA fibres, but are well below those of melt-spun polyethylene (PE), polypropylene (PP), and poly(ethylene terephthalate) (PET) with moduli ranging

from 15 to 70 GPa [20]. The reason for this is the low intrinsic modulus of a PLLA crystal. Nishino *et al.* reported the theoretical crystal moduli for a range of polymers as derived from X-ray diffraction studies. The maximum achievable moduli of PE, PP and, PET along the chain axis are 235 GPa, 40 GPa and 108 GPa, respectively, while the maximum modulus for PLLA is only 12 GPa [21,22].

3.2. The Influence of Drawing on Thermal Properties of PLLA Tapes

DSC was performed to find the development in crystallinity after drawing. As seen in Figure 4a, the as-extruded tapes were almost amorphous (4% crystallinity). The melting peaks observed are related to the crystallization developed during the DSC scan. It should be noted that for as-extruded tapes, a glass transition with an enthalpy relaxation rather than a typical step change is observed. For samples that have been stored for a long time below the T_g, the first heating curve often exhibits an endothermic relaxation peak rather than a step change. This peak can no longer be observed in the cooling curve. Preparing amorphous film is very important, because a too high initial crystallinity will reduce the maximum attainable draw ratio and consequently lower the final tape's mechanical properties. In agreement, Hyon and co-workers [23] started from as-spun fibres with crystallinity not greater than 5%, to draw them six times.

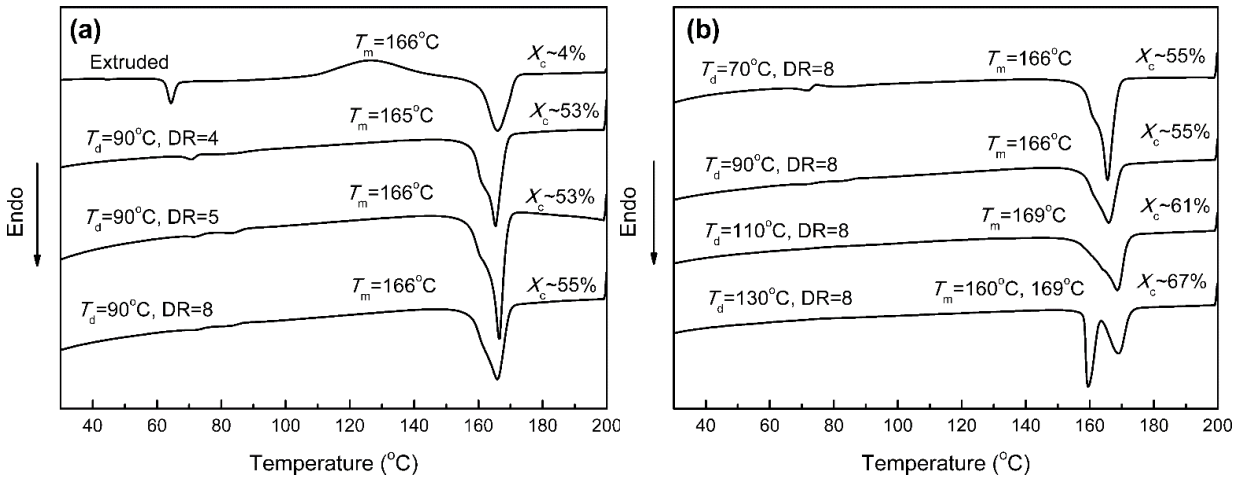

Figure 4. Differential scanning calorimetry (DSC) thermograms of (**a**) samples drawn at 90 °C with various draw ratios; and (**b**) samples drawn at different temperatures with a draw ratio of 8.

For tapes drawn at 90 °C, the crystallinity increased dramatically to 53% and then reached a plateau at $DR = 4$. The T_g and cold crystallization peaks were not detected in the DSC thermograms of drawn tapes. The melting peaks of all the samples appeared at 166 °C.

Furthermore, it is clear that increasing the drawing temperature results in a higher degree of crystallinity. The value for tapes drawn at 70 °C is 55% and rises to 67% for tapes drawn at 130 °C. Two different melting peaks can be distinguished for tapes drawn at 130 °C, at about 160 and 169 °C, respectively. The observed secondary peaks at lower temperatures are most likely due to varying lamellae thicknesses being present in the respective tapes.

Since the mechanical properties of polymers are dependent on intermolecular interactions, the performance of polymers depends on the applied strain rate and temperature of loading. The typical

DMA plots, displaying the storage modulus (E') and tan δ (E''/E') as a function of temperature, are shown in Figure 5. The mechanical glass transition is taken as the temperature of the maximum in tan δ. As seen in Figure 5a, all tapes show a similarly shaped curve. Below T_g, E' does not change much with temperature because the amorphous molecules are still essentially glassy. As soon as T_g is approached, however, the polymer chains in the amorphous phase become mobile, resulting in a reduced stiffness.

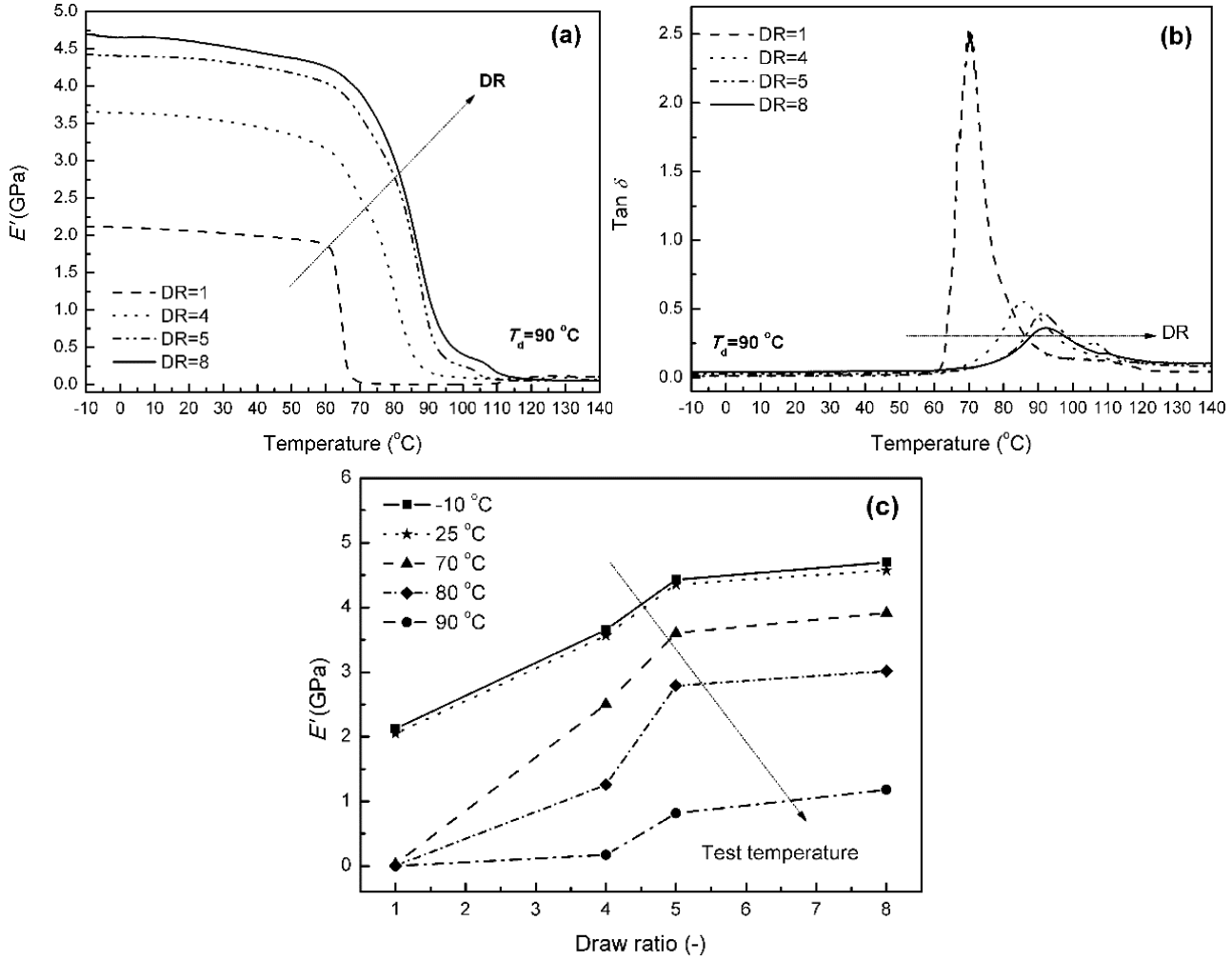

Figure 5. (**a**) Storage modulus and (**b**) loss factor against temperature for a range of PLLA tapes with increasing draw ratio; (**c**) storage modulus *vs.* draw ratio for a range of PLLA tapes with increasing test temperature.

Figure 5b shows how solid-state drawing influenced the tan δ peak position of PLLA. As we can see, the tan δ peak is shifted to higher temperatures with increased draw ratio. The peak position for PLLA was at 70.0 °C and increased to 92.2 °C for drawn tapes with DR = 8. It was reported earlier that T_g is influenced by the degree of crystallinity in PLLA [24]. Moreover, it was reported that orientation leads to a lower entropy in tapes, thus resulting in a higher T_m [25]. Similarly, upon heating, the highly ordered oriented PLLA chains in the amorphous phase will try to re-establish their preferential isotropic state. However, chains in constrained tapes have less mobility and as a result a higher T_g. Therefore, this positive shift in tan δ peak position can be attributed to strain-induced crystallization and a constrained oriented amorphous phase. Additionally, the intensity of the tanδ peak decreased with draw ratio

compared to as-extruded tapes. This indicates that fewer polymer chains are participating in this transition. It should be noted that the T_g values obtained from DMA are typically higher than those from DSC. This is because the oriented tapes studied with DSC are unconstrained and can relax before reaching T_g. Sub-T_g relaxation is inhibited for the DMA experiment because the oriented tapes are always slightly stressed. The confinement of the pre-straining prevents, or at least slows down, relaxation [25].

Moreover, E' increases with draw ratio within the temperature range studied. As seen in Figure 5c, below T_g (70–92 °C), there is no significant change in E' for all tapes when increasing the test temperature from −10 °C to 25 °C. At 80 °C, drawn tapes with DR = 4 possess a low storage modulus of approximately 1.3 GPa, which indicates that the tapes have totally relaxed. The higher stretched tapes with DR = 5 and 8, retain a higher modulus at elevated temperatures, possessing storage moduli of 2.8 GPa and 3.0 GPa respectively at 80 °C. These values shows that these tapes still possess a greater storage modulus at 80 °C than undrawn PLLA possesses at room temperature (2 GPa).

3.3. Structure Development in PLLA Tapes during Solid-State Drawing

It was shown that depending on the drawing conditions, PLLA is able to crystallize into different forms. When an amorphous film was drawn by a tensile force slightly above the T_g (60 °C), an oriented film with α crystals was obtained. When a semi-crystalline sample with α crystals was drawn, part of the α crystals are transformed into oriented β crystals, depending on the drawing conditions [26]. Eling *et al.* [9] reported that β crystals were generated upon tensile drawing at a high temperature to a higher draw ratio, whereas drawing at a low temperature and/or low draw ratio produced α crystals. Thus, the drawn products of PLLA commonly consist of β crystals or a mixture of β and α crystal. Leenslag *et al.* [8] and Hoogsteen *et al.* [27] prepared high-strength PLLA fibres that consisted of pure β-form crystals by hot drawing of solution-spun fibres at 200–204 °C, *viz*. 20–25 °C above T_m of an α crystal, to a draw ratios of 14–20. They found that the formation of β crystals depended on the sample molecular weight and molecular weight distribution in addition to the drawing temperature and draw ratio.

It is very difficult to distinguish β reflections in WAXD pattern due to the overlap with α reflections. Since only long sequences of the 3_1 helix contribute to the X-ray $(003)_\beta$ reflection and shorter ones do not contribute to the intensity of this reflection, whereas the IR band of 912 cm^{-1} is active to the 3_1 helix independent of the sequence lengths. Thus, IR spectroscopy is more sensitive to detect a small amount of β crystals within a sample [28]. Therefore, the crystal transformation upon drawing was also characterized by IR spectroscopy. Cohn *et al.* [29] reported an absorption band at 921 cm^{-1} characteristic of α crystal. On the other hand, β crystals exhibit an absorption band at 912 cm^{-1}, which is assigned to the CH_3 rocking mode of β crystals.

Figure 6 shows FT-IR spectra for a DR series prepared by solid-state drawing of PLLA at different drawing temperatures. According to the many FT-IR studies of PLLA, the band at 955 cm^{-1} is ascribed to the amorphous phase. The strong band at 871 cm^{-1} is attributed to C–C backbone stretching. No absorption peak of either α or β crystal was observed for an original as-extruded film. An absorption band at 923 cm^{-1} characteristic of α-form crystal appeared at a DR of 4. The intensity of this band became gradually stronger with increasing DR. All the samples do not show a new absorption band at 912 cm^{-1} characteristic of β-form crystal, indicating no crystal transformation obtained in this study.

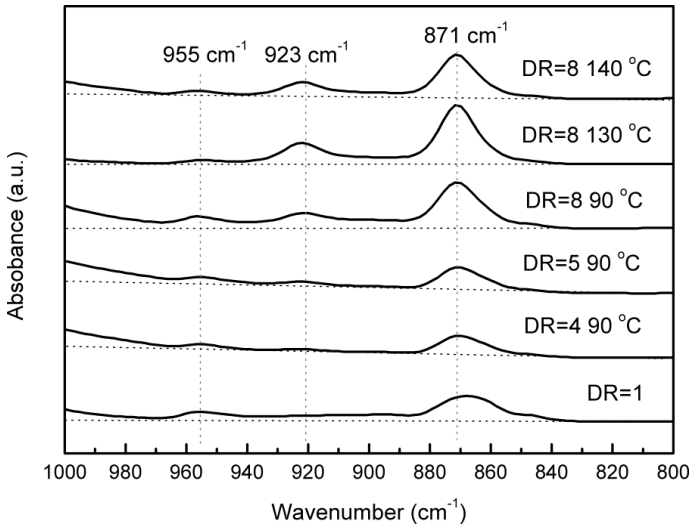

Figure 6. Infrared spectra in the 800–1000 cm^{-1} region for a series of *DR* prepared at different drawing temperature. Note the appearance of the bands at 923 and 912 cm^{-1} characteristic of α and β crystals, respectively.

2D-WAXS was performed to determine the PLLA orientation after stretching. Figure 7 displays the 2D-WAXS patterns of a *DR* series of PLLA drawn at T_d = 90 °C and also a T_d series of PLLA with *DR* = 8. Herman's orientation factor (*f*) calculated from Gaussian function, as well as the full width at half maximum (FWHM) of the (200/110) diffraction peaks are used to quantify the orientation of PLLA, and the corresponding values for various tapes are listed in Table 5.

Table 5. Crystalline orientation of various PLLA tapes obtained by Wide-angle X-ray scattering (WAXS).

T_d (°C)	*DR*	Herman's Orientation Factor* (200/110)	FWHM (200/110) (°)
90	4	0.99	7.4
90	5	0.98	9.4
90	8	0.55	16.3
130	8	0.99	5.3
140	8	0.99	6.2

Notes: * Herman's orientation factor (*f*) is given by $f = \frac{3\cos^2\theta - 1}{2}$, where θ is the angle between the orienting entity and the tape axis. Full width at half maximum (FWHM) of the (200/110) diffraction peaks is generated from the azimuthal intensity distribution. Smaller FWHM values correspond to a higher degree of orientation.

The PLLA as-extruded tape shows a diffuse isotropic scatter typical of an amorphous polymer. In the case of uniaxially drawn PLA tape with *DR* = 4, there is a rapid growth of discrete equatorial reflections with low azimuthal spread typical of a well-oriented crystalline phase. The Herman's orientation factors of PLLA tapes drawn at 90 °C are 0.99 and 0.98 for *DR* = 4 and 5, respectively. However, upon further drawing to *DR* = 8, Herman's orientation factor decreases to 0.55. This tape displays a wider azimuthal spread suggesting crystals with poorer orientation, which is an unusual phenomenon. However, occasionally this occurs when the sample is "over-drawn" at a temperature that is too low [30].

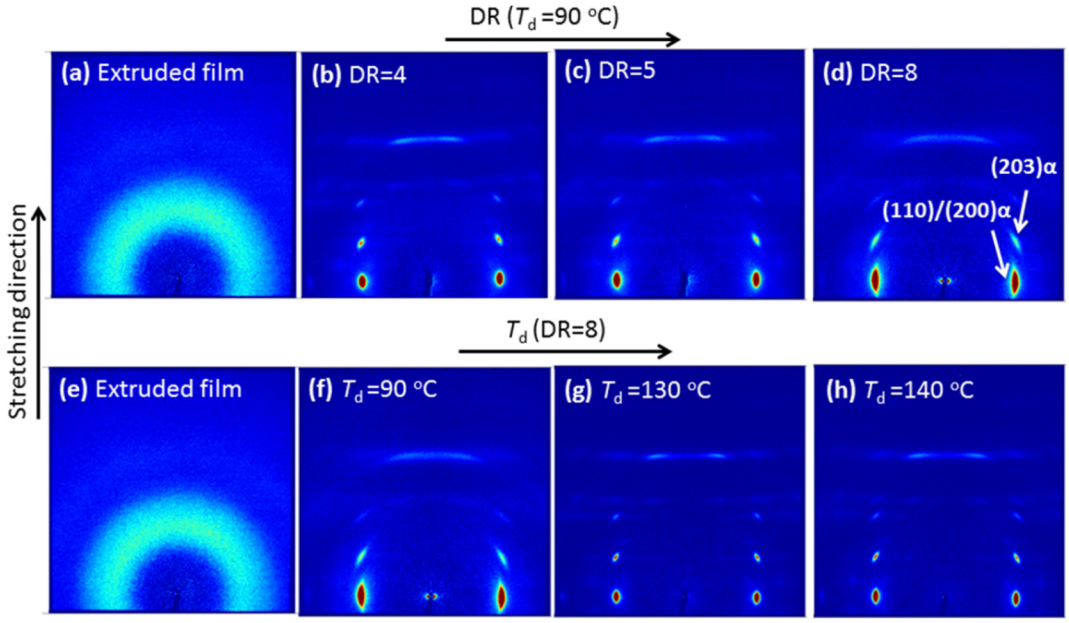

Figure 7. 2D WAXS patterns of (**a**,**e**) as-extruded tapes, tapes drawn at 90 °C to *DR* of (**b**) 4; (**c**) 5 and (**d**,**f**) 8; and PLLA tapes drawn at (**g**) 130 °C (*DR* = 8) and (**h**) 140 °C (*DR* = 8).The patterns were recorded with the incident beam perpendicular to the tapes.

An "over-drawing" regime was observed for the tape with *DR* = 8 drawn at 90 °C. It can be seen in Figure 8 that tapes drawn at *DR* = 4 and 5 are transparent while the tape drawn at *DR* = 8 is completely opaque due to the development of micro-voids during "over-drawing". SEM was also performed in order to explain this phenomenon. As seen in Figure 9, the alignment of lamellae stacks can be viewed clearly for tapes drawn at *DR* = 4. Denser packing of lamellae is found in tapes drawn at *DR* = 5. At *DR* = 8, a fibrillated structure is observed. Micro-voids align parallel to the drawing direction. Furthermore, wavy striations appear perpendicular to the tape axis. These striations are present not only at the surface of the tape but in the core as well, indicating the occurrence of crystal reassembling. Therefore, the decreased crystalline orientation observed in WAXS may be due to breakdown of the oriented structure in the "over-drawn" samples. Zhang *et al.* [31] reported that when the drawing temperature is just above T_g (75 °C), during further stretching of PLA (strain > 100%), voids and cavities appear and develop, together with the breakdown of existing crystals.

These worm-like structures have also been observed before in oriented PP tapes. Schimanski *et al.* [30] found that for PP tapes with *DR* > 10, an "over-drawing" regime existed where tapes changed from transparent to opaque. They also observed that the crystal orientation increased rapidly with increasing *DR* at first, but started to decrease for *DR* > 10.

This decrease in crystalline orientation can be avoided by increasing T_d. It can be seen in Figure 7 that the arcs transform into spots with increasing T_d, demonstrating an increase in orientation of the crystalline phase. Therefore, the improved modulus and strength with T_d can be attributed to both an increase in crystallinity, as well as orientation of the crystalline phase.

Figure 8. Optical appearance of PLLA tapes. From left to right; as-extruded tape, and tapes drawn at 90 °C to *DR* = 4, 5 and 8. There is a clear transition from fully transparent to an opaque tape structure at *DR* > 5.

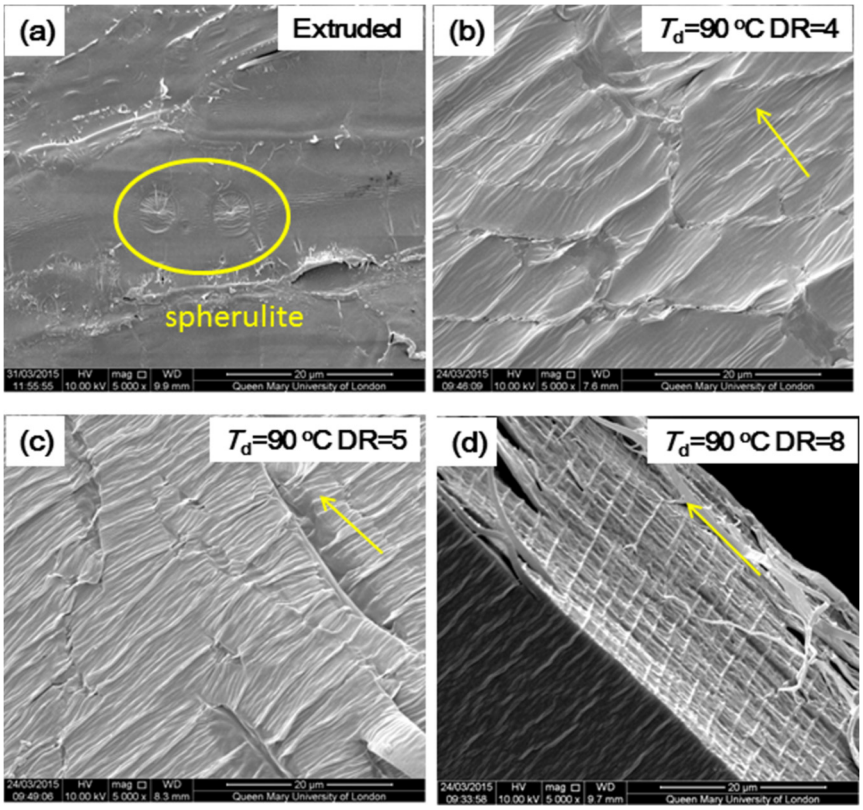

Figure 9. Scanning electron microscopy (SEM) cross-section images of (**a**) as-extruded tape and tapes drawn at 90 °C with (**b**) *DR* = 4; (**c**) *DR* = 5; and (**d**) *DR* = 8. Arrows indicate the stretching directions.

In conclusion, when the as-extruded tapes are stretched at 90 °C, structural and morphological characterization indicates strain-induced crystallization (Figure 4a) at low *DR* = 4. The orientation of the crystalline phase increases at small strains, while upon further stretching, a decrease in crystalline orientation is observed due to breakdown of existing crystals in the "overdrawing" regime. The remaining mechanical properties in these tapes (*DR* = 8) are mainly due to enhanced orientation of the amorphous phase (see T_g shift in Figure 5). For fixed draw ratios, a significant increase in Young's

modulus and tensile strength is observed with increasing drawing temperature, due to the increase in crystallinity (Figure 4b) and orientation (Figure 7) obtained for tapes drawn at higher temperatures.

3.4. Degradation Behaviour of Oriented PLLA Tapes

In previous works, numerous authors have reported extensively on the thermal degradation of PLA after melt processing. This degradation is attributed to ester group cleavage, as a consequence of the hydrolytic process at the high temperatures during melt processing in the presence of residual water [23]. In the present work, PLLA extruded films produced by melt processing showed a reduction of M_n by about 28%, from 133,500 g·mol^{-1} of pellets to about 96,100 g·mol^{-1} for as-extruded tapes. Eling *et al.* [9] produced fibres in which degradation was no higher than 40%. Fambri *et al.* [7] reported a molar mass degradation of more than 60% after melt spinning, but this result can be attributed more to shear stress effects due to long residence times.

It has been found that the degradability of PLA can be modified significantly by changing the microstructure of the polymer. Figure 10 presents the GPC results of undrawn and drawn PLA tapes before and after degradation in two mediums at 50 °C. The results show that drawing has a significant effect on the hydrolytic degradation. In both mediums, the extent of degradation was lower for drawn tapes than for as-extruded tapes. For example, after degradation for four weeks in water, the molecular weight of the tape with DR = 8 is about twice that of isotropic films.

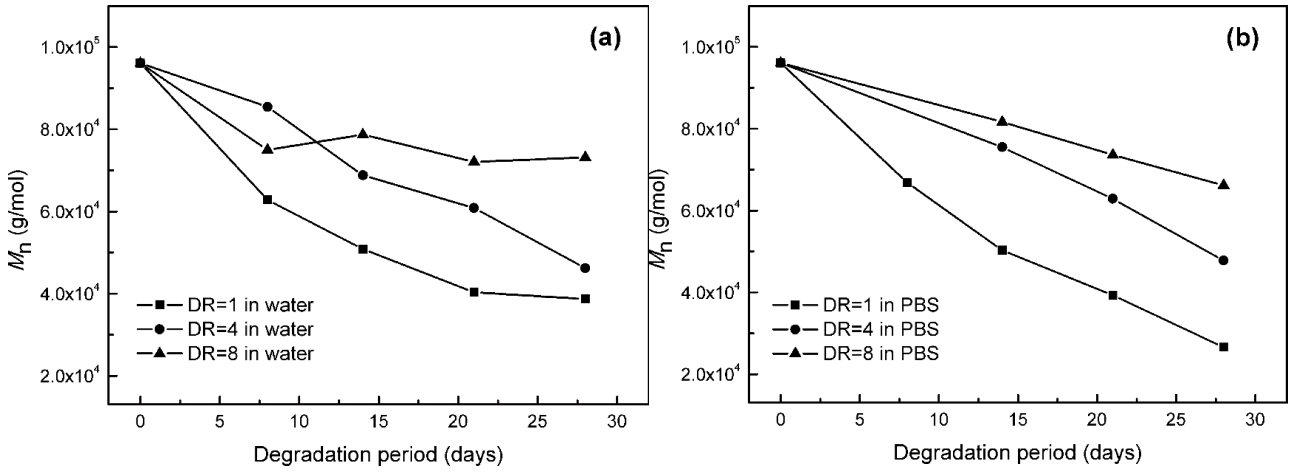

Figure 10. Residual molecular weights of PLLA as-extruded and drawn tapes before and after degradation in (**a**) water and (**b**) PBS.

It is well established that biodegradation of semi-crystalline polymers first occurs in the disordered amorphous phase. Rangari and Vasanthan [32] reported that the highest percentage of weight loss was observed for films with the lowest initial crystallinity, indicating that the extent of degradation decreases with increasing crystallinity. Moreover, this amorphous component can include a restricted amorphous and free amorphous phase, where the degradation rate of the restricted amorphous component is usually much slower compared to the free amorphous component [32].

It is not easy to fully analyse how the microstructure affects the hydrolytic degradation of PLLA because the crystallinity as well as molecular orientation in both amorphous and crystalline phase changes with drawing. For example, as shown in the DSC, DMA and WAXS data earlier, the as-extruded

tape has a very low crystallinity of 4% and an isotropic structure. On the other hand, in tapes of $DR = 8$, the crystallinity increases to 55%, while at the same time the crystalline domains orient ($f = 0.55$). Besides, the increase in T_g (from 70 °C for the former to 92 °C for the latter) indicates a more constrained oriented amorphous phase after drawing. Therefore, it is hard to determine which factor plays the dominant role in lowering the degradation rate.

However, if we compare the tapes of $DR = 4$ with those of $DR = 8$, approximately 52% of molecular loss occurred for tapes with $DR = 4$ after four weeks of degradation in water and only 24% of molecular loss was observed for tapes with $DR = 8$ during the same time period. The crystallinity of the former (53%) is very close to that of the latter (55%), while the Herman's orientation factor of the former ($f = 0.99$) is greater than that of the latter ($f = 0.55$). Higher T_g values (92 °C) were observed for $DR = 8$ than at $DR = 4$ (85 °C), suggesting higher orientation of the amorphous phase. Therefore, we may conclude that the restricted amorphous phase in this case plays a dominant role in slowing down the degradation.

In summary, solid-state drawing has a significant effect on the hydrolytic degradation behaviour of PLA due to the morphological changes. Therefore, it can be useful for tailoring the degradability of PLA products.

4. Conclusions

The drawing conditions of PLLA determine the morphology of the polymer, and through this control their mechanical properties and degradation profile. Both draw ratio and drawing temperature play an important role in the polymer morphology and resulting properties of PLLA tapes. An increase in modulus and strength is seen with increasing draw ratio, due to strain-induced crystallization and orientation. More importantly a large increase in toughness was observed with drawing, which is highly relevant for numerous PLLA film applications. Drawing at higher temperatures increases the modulus and strength further, which accounts for the improved orientation and crystallinity. In all tapes, α-form crystals were observed. Such highly oriented PLLA tapes of high tensile strength, modulus, and toughness, are of interest for composite applications and can when combined with isotropic PLLA films lead to the creation of biobased, fully recyclable, self-reinforced PLLA composites [33].

Acknowledgments

This research was funded by the European Commission's (EC) MATERA+ program (project HIGHBIOPOL) with support from the DG06 (Région Wallonne) and the Technology Strategy Board (TSB) (Wiltshire, UK). We would like to thank Takashi Nishino at Kobe University for helpful discussions. Fang Mai would like to acknowledge financial support through the China Scholarship Council (CSC).

Author Contributions

Ton Peijs and Fang Mai designed the experiments. Ton Peijs and Fang Mai directed the research. Fang Mai and Wei Tu performed the experiments. Fang Mai wrote the manuscript. All authors discussed the results and edited the manuscript.

Conflicts of Interest

The authors declare no conflict of interest.

References

1. Berglund, L.A.; Peijs, T. Cellulose biocomposites—From bulk moldings to nanostructured systems. *MRS Bull.* **2010**, *35*, 201–207.
2. Murariu, M.; Dechief, A.; Ramy-Ratiarison, R.; Paint, Y.; Raquez, J.; Dubois, P. Recent advances in production of poly(lactic acid) (PLA) nanocomposites: A versatile-method to tune crystallization properties of PLA. *Nanocomposites* **2015**, *1*, 71–82.
3. Ward, I. Developments in oriented polymers, 1970–2004. *Plast Rubber Compos.* **2004**, *33*, 189–194.
4. Smith, P.; Lemstra, P.J. Ultra-high-strength polyethylene filaments by solution spinning/drawing. *J. Mater. Sci.* **1980**, *15*, 505–514.
5. Kwolek, S.; Morgan, P.; Schaefgen, J.; Gulrich, L. Synthesis, anisotropic solutions, and fibers of poly(1,4-benzamide). *Macromolecules* **1977**, *10*, 1390–1396.
6. Penning, J.; Dijkstra, H.; Pennings, A. Preparation and properties of absorbable fibres from L-lactide copolymers. *Polymer* **1993**, *34*, 942–951.
7. Fambri, L.; Pegoretti, A.; Mazzurana, M.; Migliaresi, C. Biodegradable fibres. *J. Mater. Sci. Mater. Med.* **1994**, *5*, 679–683.
8. Leenslag, J.; Pennings, A. High-strength poly(L-lactide) fibres by a dry-spinning/hot-drawing process. *Polymer* **1987**, *28*, 1695–1702.
9. Eling, B.; Gogolewski, S.; Pennings, A. Biodegradable materials of poly(L-lactic acid): 1. Melt-spun and solution-spun fibres. *Polymer* **1982**, *23*, 1587–1593.
10. Cicero, J.A.; Dorgan, J.R. Physical properties and fiber morphology of poly(lactic acid) obtained from continuous two-step melt spinning. *J. Polym. Environ.* **2001**, *9*, 1–10.
11. Cicero, J.A.; Dorgan, J.R.; Janzen, J.; Garrett, J.; Runt, J.; Lin, J. Supramolecular morphology of two-step, melt-spun poly(lactic acid) fibers. *J. Appl. Polym. Sci.* **2002**, *86*, 2828–2838.
12. Mezghani, K.; Spruiell, J. High speed melt spinning of poly(L-lactic acid) filaments. *J. Polym. Sci. Part B Polym. Phys.* **1998**, *36*, 1005–1012.
13. Rangari, D.; Vasanthan, N. Study of strain-induced crystallization and enzymatic degradation of drawn poly(L-lactic acid) (PLLA) films. *Macromolecules* **2012**, *45*, 7397–7403.
14. Oh, M.O.; Kim, S.H. Conformational development of polylactide films induced by uniaxial drawing. *Polym. Int.* **2014**, *63*, 1247–1253.
15. Alcock, B.; Cabrera, N.O.; Barkoula, N.M.; Peijs, T. The effect of processing conditions on the mechanical properties and thermal stability of highly oriented PP tapes. *Eur. Polym. J.* **2009**, *45*, 2878–2894.
16. Grijpma, D.W.; Altpeter, H.; Bevis, M.J.; Feijen, J. Improvement of the mechanical properties of poly(D,L-lactide) by orientation. *Polym. Int.* **2002**, *51*, 845–851.
17. Söntjens, S.H.M.; Engels, T.A.P.; Smit, T.H.; Govaert, L.E. Time-dependent failure of amorphous poly-D,L-lactide: Influence of molecular weight. *J. Mech. Behav. Biomed.* **2012**, *13*, 69–77.

18. Meijer, H.E.H.; Govaert, L.E. Mechanical performance of polymer systems: The relation between structure and properties. *Prog. Polym. Sci.* **2005**, *30*, 915–938.
19. Van Melick, H.G.H.; Govaert, L.E.; Meijer, H.E.H. Localisation phenomena in glassy polymers: Influence of thermal and mechanical history. *Polymer* **2003**, *44*, 3579–3591.
20. Alcock, B.; Peijs, T. Polymer Composites—Polyolefin Fractionation—Polymeric Peptidomimetics-Collagens; Springer: Heidelberg, Germany, 2013; pp. 1–76.
21. Nishino, T.; Takano, K.; Nakamae, K. Elastic modulus of the crystalline regions of cellulose polymorphs. *Polym. Sci. Part B Polym. Phys.* **1995**, *33*, 1647–1651.
22. Crist, B. The ultimate strength and stiffness of polymers. *Annu. Rev. Mater. Sci.* **1995**, *25*, 295–323.
23. Hyon, S.H.; Jamshidi, K.; Ikada, Y. *Polymers as Biomaterials*; Springer: New York, NY, USA, 1984; pp. 51–65.
24. Gupta, B.; Revagade, N.; Hilborn, J. Poly(lactic acid) fiber: An overview. *Prog. Polym. Sci.* **2007**, *32*, 455–482.
25. Barkoula, N.M.; Peijs, T.; Schimanski, T.; Loos, J. Processing of single polymer composites using the concept of constrained fibers. *Polym. Compos.* **2005**, *26*, 114–120.
26. Kalb, B.; Pennings, A. General crystallization behaviour of poly(L-lactic acid). *Polymer* **1980**, *21*, 607–612.
27. Hoogsteen, W.; Postema, A.; Pennings, A.; Ten Brinke, G.; Zugenmaier, P. Crystal structure, conformation and morphology of solution-spun poly(L-lactide) fibers. *Macromolecules* **1990**, *23*, 634–642.
28. Sawai, D.; Takahashi, K.; Sasashige, A.; Kanamoto, T.; Hyon, S.H. Preparation of oriented β-form poly(L-lactic acid) by solid-state coextrusion: Effect of extrusion variables. *Macromolecules* **2003**, *36*, 3601–3605.
29. Cohn, D.; Younes, H. Biodegradable PEO/PLA block copolymers. *J. Biomed. Mater. Res.* **1988**, *22*, 993–1009.
30. Schimanski, T.; Loos, J.; Peijs, T.; Alcock, B.; Lemstra, P.J. On the overdrawing of melt-spun isotactic polypropylene tapes. *J. Appl. Polym. Sci.* **2007**, *103*, 2920–2931.
31. Zhang, X.; Schneider, K.; Liu, G.; Chen, J.; Brüning, K.; Wang, D.; Stamm, M. Structure variation of tensile-deformed amorphous poly(L-lactic acid): Effects of deformation rate and strain. *Polymer* **2011**, *52*, 4141–4149.
32. Vasanthan, N.; Gezer, H. Thermally induced crystallization and enzymatic degradation studies of poly(L-Lactic acid) films. *J. Appl. Polym. Sci.* **2013**, *127*, 4395–4401.
33. Mai, F.; Tu, W.; Bilotti, E.; Peijs, T. Preparation and properties of self-reinforced poly(lactic acid) composites based on oriented tapes. *Compos. Part A* **2015**, *76*, 145–153.